



Soluble syntaxin 3 functions as a transcriptional regulator

Received for publication, November 16, 2017, and in revised form, February 20, 2018. Published, Papers in Press, February 23, 2018, DOI 10.1074/jbc.RA117.000874

Adrian J. Giovannone^{‡1}, Christine Winterstein^{‡1,2}, Pallavi Bhattaram^{‡3}, Elena Reales^{‡4}, Seng Hui Low[‡], Julie E. Baggs[§], Mimi Xu[‡], Matthew A. Lalli[‡], John B. Hogenesch^{¶1}, and Thomas Weimbs^{‡5}

From the [‡]Department of Molecular, Cellular, and Developmental Biology and Neuroscience Research Institute, University of California, Santa Barbara, California 93106-9625, the [§]Department of Systems Pharmacology and Translational Therapeutics, Perelman School of Medicine, University of Pennsylvania, Philadelphia, Pennsylvania 19104, and the [¶]Center for Chronobiology, Cincinnati Children's Hospital Medical Center, Cincinnati, Ohio 45229

Edited by Phyllis I. Hanson

Syntaxins are a conserved family of SNARE proteins and contain C-terminal transmembrane anchors required for their membrane fusion activity. Here we show that Stx3 (syntaxin 3) unexpectedly also functions as a nuclear regulator of gene expression. We found that alternative splicing creates a soluble isoform that we termed Stx3S, lacking the transmembrane anchor. Soluble Stx3S binds to the nuclear import factor RanBP5 (RAN-binding protein 5), targets to the nucleus, and interacts physically and functionally with several transcription factors, including ETV4 (ETS variant 4) and ATF2 (activating transcription factor 2). Stx3S is differentially expressed in normal human tissues, during epithelial cell polarization, and in breast cancer *versus* normal breast tissue. Inhibition of endogenous Stx3S expression alters the expression of cancer-associated genes and promotes cell proliferation. Similar nuclear-targeted, soluble forms of other syntaxins were identified, suggesting that nuclear signaling is a conserved, novel function common among these membrane-trafficking proteins.

The SNARE superfamily consists of several protein families that are related to each other by the presence of one or two conserved ~60-residue-long SNARE motifs (1, 2). To mediate membrane fusion, membrane-associated cognate SNAREs interact with each other via their SNARE motifs to form highly stable SNARE complexes. This complex formation is thought to provide the driving force for membrane fusion.

This work was supported by National Institutes of Health Grant DK095248 and DK62338 (to T.W.); NINDS, National Institutes of Health Grant 1R01NS054794 (to J. B. H.); and NHBLI, National Institutes of Health Grant 1R01HL097800 (to J. B. H.); funds from the California Cancer Research Coordinating Committee (to T. W.); and postdoctoral fellowships from the Cancer Center of Santa Barbara (to C. W.) and the Spanish Ministry of Education and Science (to E. R.). The authors declare that they have no conflicts of interest with the contents of this article. The content is solely the responsibility of the authors and does not necessarily represent the official views of the National Institutes of Health.

This article contains Figs. S1–S4.

¹ Both authors contributed equally to this work.

² Present address: Biogen GmbH, 85737 Ismaning, Germany.

³ Present address: Dept. of Cell Biology, Lerner Research Institute, Cleveland Clinic, Cleveland, OH 44195.

⁴ Present address: Centro de Biología Molecular Severo Ochoa, Consejo Superior de Investigaciones Científicas and Universidad Autónoma de Madrid, Cantoblanco, 28049 Madrid, Spain.

⁵ To whom correspondence should be addressed: Dept. of Molecular, Cellular & Developmental Biology, University of California Santa Barbara, Santa Barbara, CA 93106-9625. E-mail: weimbs@ucsb.edu.

The crucial role of SNAREs in membrane fusion is well accepted, and many mechanistic and regulatory details are well understood (3–5).

Members of the Stx (syntaxin) family of SNAREs are central to all SNARE complexes and contain a C-terminal transmembrane domain, one copy of the SNARE motif, and an N-terminal three-helix bundle (1, 2). The human genome encodes at least 16 syntaxins that localize to their specific membrane domains or organelles to mediate membrane fusion reactions (6). For example, Stx1A and Stx1B are involved in synaptic vesicle fusion during neurotransmitter release (4), whereas Stx3 localizes to the apical plasma membrane domains of polarized epithelial cells (7–10), functions in polarized trafficking pathways, and is essential to the correct establishment of cell polarity (11–14).

We report here the unexpected discovery of a novel function of Stx3—and likely many other Stx family members—as a regulator of gene expression in the nucleus. We show that a soluble form of Stx3 is generated by alternative RNA splicing. This non-membrane-anchored Stx3 isoform (termed Stx3S) interacts with the nuclear import factor RanBP5, undergoes nuclear translocation, and binds to and regulates several transcription factors including the ETS domain transcription factor ETV4 (also known as Pea3 or E1AF) and the leucine zipper family transcription factor ATF2. Both ETV4 and ATF2 are implicated in carcinogenesis and metastasis (15, 16). The Stx3S splice variant is endogenously expressed in human tissues *in vivo* and in several cell lines in culture. Its expression is up-regulated during polarization of human colon adenocarcinoma cells, and down-regulated in triple-negative breast cancer samples compared with normal human breast samples, suggesting a possible role in carcinogenesis. Inhibition of endogenous Stx3S expression leads to changes in cellular gene expression and promotes cell proliferation.

Our results demonstrate that this novel isoform of Stx3 can act as a transcriptional regulator. In addition to Stx3, several other syntaxin family members also undergo similar alternative splicing events leading to non-membrane-anchored forms, suggesting that nuclear regulatory functions are conserved among SNAREs of the syntaxin family. These results suggest the existence of previously unrecognized signaling mechanisms that may directly link membrane-trafficking pathways with the regulation of gene expression.

Results

Nuclear targeting of Stx3

To identify new Stx3 interaction partners, co-immunoprecipitation experiments were performed using C-terminally Myc-epitope-tagged Stx3 stably transfected in the MDCK renal epithelial cell line under the control of a doxycycline (DOX)-inducible⁶ promoter (14). In addition to the anticipated, known Stx3-binding partner munc-18b (Fig. 1A, band b), a protein with a relative molecular mass of 110 kDa (band a) co-precipitated with Stx3 (band c). By mass spectrometry (Fig. S1), this protein was identified as the nuclear import factor RanBP5, also known as karyopherin β 3, importin β 3, or importin 5 (17). Interaction between exogenous Myc-tagged Stx3 and endogenous RanBP5 was verified by reciprocal co-immunoprecipitation (Fig. 1, B and C).

Using Stx3 deletion constructs (Fig. 1D), the N-terminal three-helix bundle of Stx3 was identified as the necessary and sufficient RanBP5-interacting domain (Fig. 1, E and F). The apparent strength of the Stx3-RanBP5 interaction increases if the three-helix bundle of Stx3 is expressed in isolation, either in a soluble form (amino acids 1–146) or a membrane-anchored form (amino acids 27–146 + transmembrane domain) (Fig. 1, E and F). Syntaxins are known to adopt a “closed” conformation in which the three-helix bundle folds back onto the SNARE domain to form an intramolecular helical bundle. In this conformation, syntaxins are unable to interact with other SNARE partners. In contrast, in the “open” conformation, the three-helix bundle is free, and syntaxins can engage in SNARE interaction (18–20). To determine whether RanBP5 favors the open conformation of Stx3, the L165A/E166A mutation was introduced, which locks Stx3 in its open conformation (21). As shown in Fig. 1G, the open mutation enhances the interaction of Stx3 with RanBP5. Altogether, these results indicate that the nuclear import factor RanBP5 interacts with the three-helix bundle motif of Stx3 and that this interaction preferentially occurs when this motif is not engaged in interactions with Stx3's SNARE motif.

We hypothesized that the interaction with RanBP5 may result in import of Stx3 into the nucleus provided that Stx3 is not membrane-anchored. To test this, membrane-anchored Stx3A and several soluble constructs lacking the membrane anchor were expressed in MDCK cells. Consistent with previously results (7, 9, 14), membrane-anchored Stx3A localizes to the plasma membrane and intracellular vesicles (Fig. 1H, panel a). Soluble Stx3 constructs that contain the three-helix bundle but lack the transmembrane anchor concentrate in the nucleoplasm, suggesting active nuclear import (Fig. 1H, panels b–d). Furthermore, a membrane-anchored mutant of Stx3 that is lacking the SNARE domain (Stx3(1–146-TM)) is prominently targeted to the nuclear envelope, in addition to other locations, but not the nucleoplasm (Fig. 1H, panel e). These observations suggest that Stx3 is actively transported to the nucleoplasm,

presumably *via* its interaction with RanBP5, provided it is not membrane-anchored.

Alternative splicing leads to a Stx3 isoform lacking the transmembrane domain

Because Stx3 is an integral membrane protein, the finding of nucleoplasmic targeting could only be of plausible significance if the membrane anchor of Stx3 was absent. Isoforms derived from alternative splicing of several syntaxins have been reported (22, 23), including some that lack apparent transmembrane domains (24), but their relevance or function have remained unknown. We used BLAST to search for cDNAs of potential novel isoforms of human Stx3 in expressed sequence tag (EST) databases. Several ESTs supported the existence of an isoform lacking exon 10 (Fig. 2A). This would lead to the loss of the transmembrane domain and expression of a truncated, soluble protein containing a unique C-terminal 12-residue peptide (Fig. 2B). We termed this novel isoform Stx3S (Stx3 Soluble). Expression of Stx3S was confirmed by RT-PCR from human embryonic kidney cells (HEK293T) (Fig. 2C) and DNA sequencing of the amplified cDNA fragments, and the full-length cDNA of Stx3S was isolated and cloned. RT-PCR analysis of normal human kidney revealed that Stx3S is expressed in addition to membrane-anchored Stx3A (Fig. 2D).

To confirm that Stx3S is expressed endogenously at the protein level, an antibody against its unique C-terminal peptide was generated and tested in a panel of human cell lines. Endogenous Stx3S protein is detectable in HEK293T and Caco2 cells (Fig. 2E) consistent with mRNA expression in these cell lines (Fig. 2, C and J). Targeting an mRNA region common between Stx3A and Stx3S by shRNA diminishes expression of both Stx3 and Stx3S, confirming specificity of the protein signal (Fig. 2E). At the endogenous protein level, Stx3S is expressed much lower than Stx3A and only detectable after enrichment by immunoprecipitation (Fig. 2E).

Using an *in vitro* binding assay, we verified that Stx3S readily interacts with RanBP5 (Fig. 2F) and, using our expression plasmid, targets to the nucleoplasm (Fig. 2G). Inhibition of CRM1/exportin 1 with the nuclear export inhibitor leptomycin B (25) leads to increased nuclear accumulation of Stx3S, suggesting that Stx3S undergoes CRM1-dependent nuclear-cytoplasmic shuttling. Treatment with the proteasome inhibitor ALLN results in significantly elevated expression levels (Fig. 2, I and J), suggesting that Stx3S is subject to proteasomal degradation. Even at the lowest detectable expression levels, Stx3S accumulates in the nucleoplasm (Fig. 2J), indicating that its nuclear localization is not a consequence of overexpression.

Altogether, these results indicate that Stx3S is a novel isoform of Stx3 generated by alternative splicing leading to a non-membrane-anchored, nuclear-targeted protein. The Stx3S mRNA is abundantly expressed in human tissue and cell lines, but the protein undergoes fast turnover compared with Stx3A.

Regulation of Stx3S expression

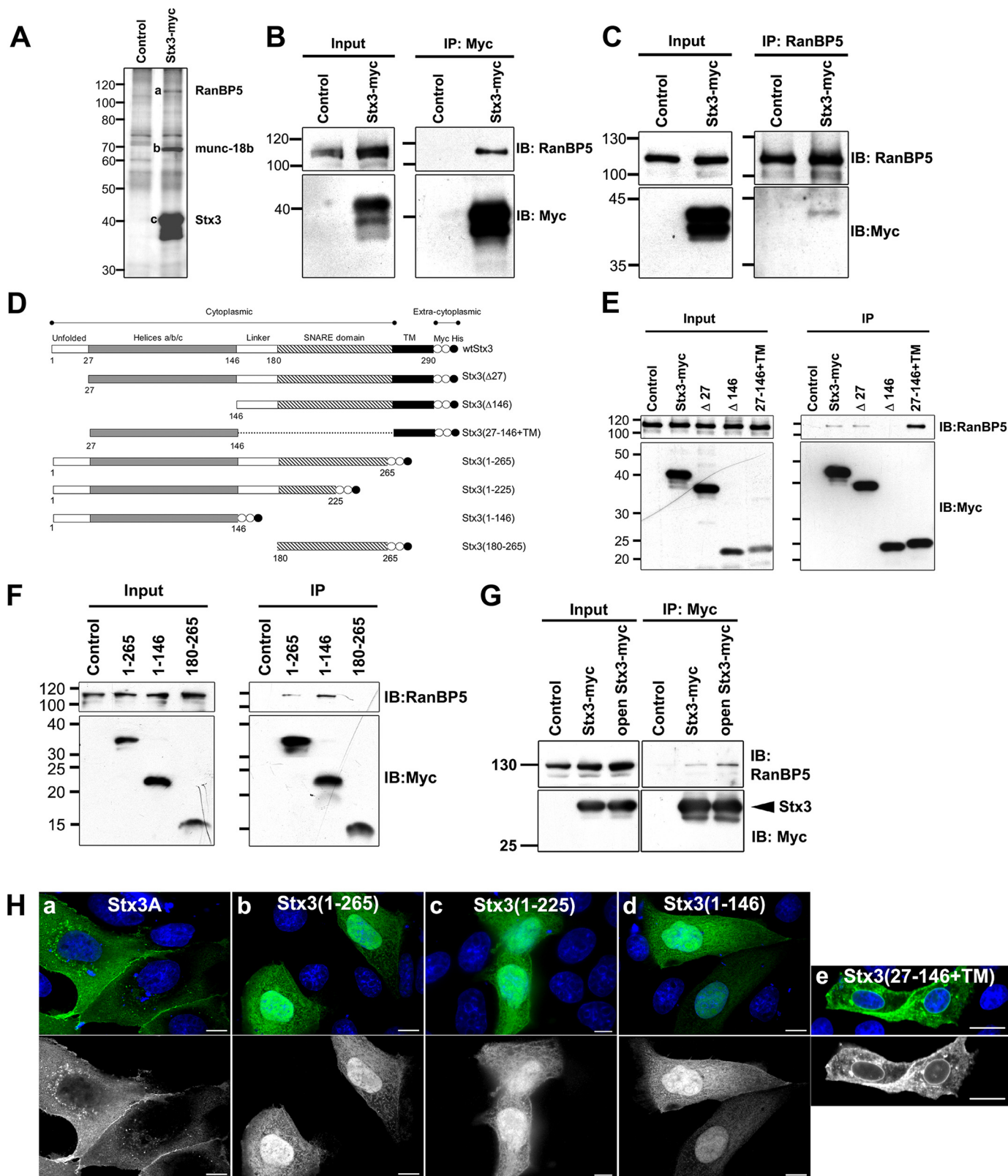
To test whether expression of endogenous Stx3S may be regulated during cell differentiation, we used the colon ac-

⁶ The abbreviations used are: DOX, doxycycline; MDCK, Madin–Darby canine kidney; EST, expressed sequence tag; NBS, normal breast sample; TNBC, triple-negative breast cancer; qPCR, quantitative PCR; FNTA, farnesyltransferase α ; DAPI, 4',6'-diamino-2-phenylindole.

Syntaxin 3 as transcriptional regulator

cinoma cell line Caco2, which is frequently used in the study of epithelial cell polarity. As these cells progress past confluence, they establish cell–cell junctions and various features of polarized morphology that are well described in the literature (26, 27). Expression levels of Stx3A *versus* Stx3S were

monitored at different time points during the establishment of polarized epithelial morphology. In contrast to Stx3A, which does not show a difference in expression during polarization, Stx3S mRNA is up-regulated after day 2 and maintains its expression level thereafter (Fig. 3A). At the protein



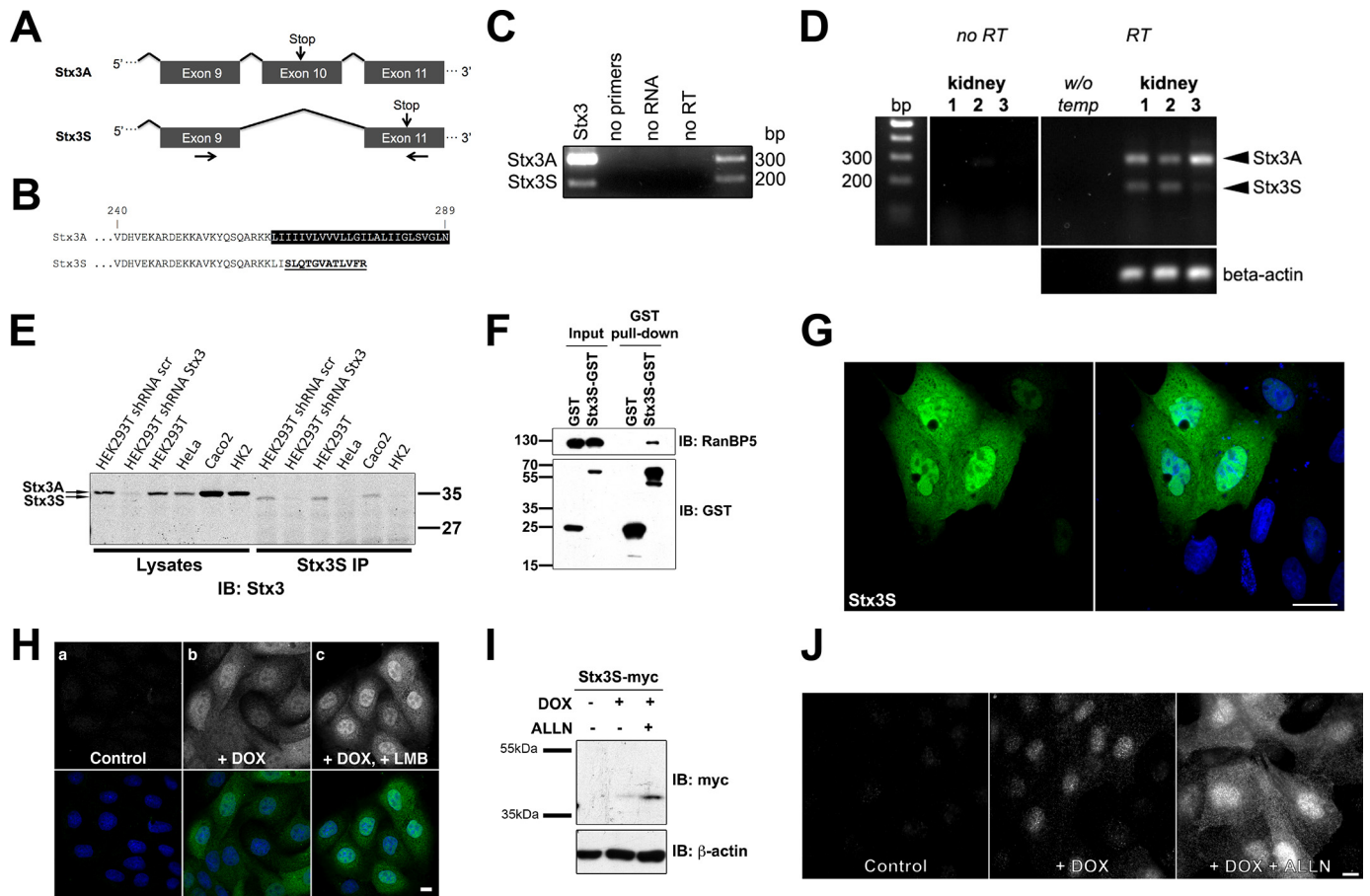


Figure 2. Identification of a novel splice-isoform of Stx3. *A*, schematic of exons 9 to 11 of the human Stx3 gene. Arrows mark primer pair used for RT-PCR in Figs. 2 (*C* and *D*) and 3*A*. *B*, amino acid alignment of the C-terminal region of Stx3A and Stx3S. *C* and *D*, RT-PCR showing bands derived from endogenous Stx3A and Stx3S transcripts in HEK293T cells (*C*) or in normal human kidney tissue from three different individuals (*D*). *E*, immunoprecipitation of endogenously expressed Stx3S in various human cell lines (HEK293T, HeLa, Caco2, and HK2) and in HEK293T cells stably expressing shRNA against all Stx3 isoforms versus HEK293T cells stably expressing scrambled (*scr*) control shRNA. Total cell lysates or immunoprecipitates (*IP*) using an Stx3S-specific antibody were analyzed by immunoblot using an anti-Stx3 antibody. The expected size shift difference between Stx3A and Stx3S is observed. *F*, co-precipitation experiment of GST–Stx3S transiently expressed in HEK293T cells demonstrates binding to endogenous RanBP5. *G*, immunocytochemistry of MDCK cells transiently expressing Myc-tagged Stx3S. Stx3S is stained using an anti-Myc antibody (green); nuclei are stained with DAPI (blue). Scale bar, 5 μ m. *H*, immunocytochemistry of MDCK cells stably expressing Myc-tagged Stx3S under DOX control. The cells were either untreated (*panel a*), treated with DOX for 24 h (*panel b*), or treated with DOX for 21 h followed by DOX + 10 ng/ml leptomycin B for 3 h (*panel c*). Stx3S is stained using an anti-Myc antibody (gray in top row and green in merged images in bottom row); nuclei are stained with DAPI (blue in bottom row). *I*, MDCK cells stably transfected for Myc-tagged Stx3S were induced with DOX or uninduced and were treated for 16 h with the proteasome inhibitor ALLN (10 μ M). Total cell lysates were analyzed by immunoblot against the Myc tag demonstrating stabilization of Stx3S after proteasomal inhibition. *J*, immunocytochemistry of induced or uninduced stably expressing Stx3S MDCK cells treated for 16 h with ALLN (10 μ M). Scale bar, 5 μ m.

level, the up-regulation of Stx3S is even more pronounced with Stx3S protein detectable at day 6 but not at day 3 (Fig. 3*B*).

To investigate whether alternative splicing between Stx3A and Stx3S may also be regulated *in vivo* and may play a role in disease, the expression profiles of Stx3 were examined in transcriptomes from human normal breast samples (NBSS)

and triple-negative breast cancer (TNBC) (28, 29). Examination of RNA sequencing reads aligning to splice junctions specific to Stx3A (exon 10/11 junction) and Stx3S (exon 9/11 junction) transcripts, respectively, revealed a notable depletion of Stx3S in TNBC relative to normal samples (Fig. 3*C*). A relative increase in the usage of the Stx3A-specific exon 10 was detected in TNBC samples, indicating a corresponding

Figure 1. Stx3 binds to RanBP5 and targets to the nucleus. *A*, Myc-tagged Stx3A was immunoprecipitated from lysates of stably transfected MDCK cells or control MDCK cells. Precipitated proteins were separated by SDS-PAGE and visualized by silver staining. Specific bands *a*, *b*, and *c* were identified by mass spectrometry as RanBP5, Munc18b, and Stx3, respectively. *B* and *C*, immunoblots showing co-immunoprecipitation experiments using stably transfected MDCK cells expressing Myc-tagged Stx3A or control MDCK cells. Immunoprecipitation was with anti-Myc antibody (*B*) or anti-RanBP5 antibody (*C*). Immunoblots were probed for endogenous RanBP5 or Myc as indicated. *D*, schematic drawing of Stx3 and all deletion constructs used in this study including nomenclature. Myc epitope tags are indicated as white circles, and His₆ tags are indicated as black circles. *E* and *F*, immunoblots of co-immunoprecipitation experiments with lysates of MDCK cells transiently expressing Myc-tagged Stx3 and Stx3 deletion constructs as indicated. Membrane-anchored (*E*) and soluble (*F*) Stx3 constructs were immunoprecipitated using an anti-Myc antibody. Interacting, endogenous RanBP5 was detected by immunoblot using an anti-RanBP5 antibody. *G*, lysates from HEK293T cells transiently transfected with Myc-tagged Stx3A or the open mutant Stx3(L165A/E166A). *H*, immunofluorescence microscopy of MDCK cells transiently expressing the indicated Myc-tagged Stx3 forms. Top row, Stx3 is stained using an anti-Myc antibody (green), and nuclei are stained with DAPI (blue). Bottom row, Stx3 channel only. Scale bars, 5 μ m for panels *a*–*d* and 10 μ m for panel *e*. *IP*, immunoprecipitation. *IB*, immunoblot.

Syntaxin 3 as transcriptional regulator

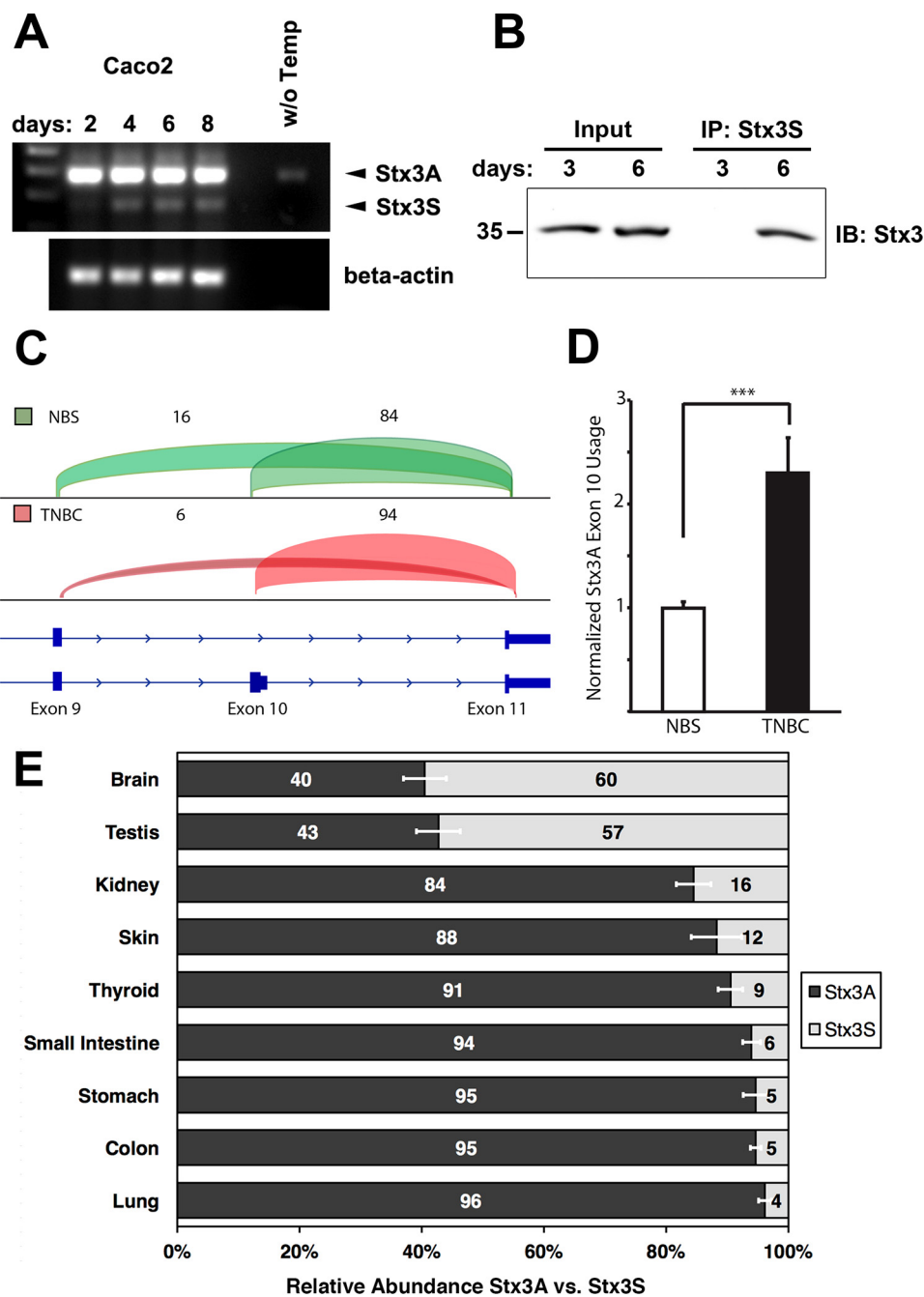


Figure 3. Regulation of Stx3S expression. *A*, Caco2 cells were cultured for the indicated durations and analyzed by RT-PCR for Stx3A/Stx3S mRNA expression using the primer pair shown in Fig. 2*A*. The endogenous Stx3S transcript is notably up-regulated during the transition from a subconfluent, highly proliferative culture (day 2) to confluent and postconfluent cultures (later days). *B*, immunoprecipitation (IP) of endogenous Stx3S with Stx3S-specific antibody from Caco2 cells cultured for indicated days. Immunoblot (IB) used total Stx3 antibody. The IP lanes are 20 \times enriched over the input lanes. Therefore, only the more abundant Stx3A is visible in the input lanes. *C*, genome browser view of transcriptome analysis of Stx3 transcripts in TNBC compared with NBSs. $n_{\text{NBS}} = 3$, $n_{\text{TNBC}} = 6$. Transcripts containing the exon 10/11 junction are unique to Stx3A, whereas transcripts containing the exon 9/11 junction are unique to Stx3S. The percentages of reads mapping to junctions 9/11 and 10/11, respectively, are indicated by numbers and visualized by brackets of heights proportional to their abundance. Stx3S is notably down-regulated, compared with Stx3A, in TNBC. *D*, normalized Stx3A exon 10 usage in RNA sequencing analysis of TNBC compared with NBSs shows relative enrichment of Stx3A versus Stx3S in TNBC, indicating again that Stx3S is down-regulated in TNBC. $n_{\text{NBS}} = 3$, $n_{\text{TNBC}} = 6$. The data are shown as means \pm S.E. ***, $p < 0.001$. Statistical analysis was performed using DEXSeq package. *E*, relative Stx3A versus Stx3S isoform expression based on analysis of splice junction usage from RNA sequencing data of multiple normal human tissues. The data are shown as the means \pm S.E.

down-regulation of Stx3S (Fig. 3*D*). This indicates that expression of Stx3S is down-regulated in TNBC.

Examining transcriptomes of various normal human tissues also revealed striking differences in the alternative mRNA splicing leading to Stx3S versus Stx3A transcripts (Fig. 3*E*). Tissues with the largest relative expression of Stx3S are testis

and brain, with over 50% of the Stx3 transcript population. This is in contrast to other tissues, e.g. lung, which exhibits a drastically lower abundance of Stx3S mRNA at 4%. Altogether, these results indicate that Stx3S is a widely expressed isoform whose expression is controlled by tissue-specific regulation of alternative RNA splicing and is down-regulated

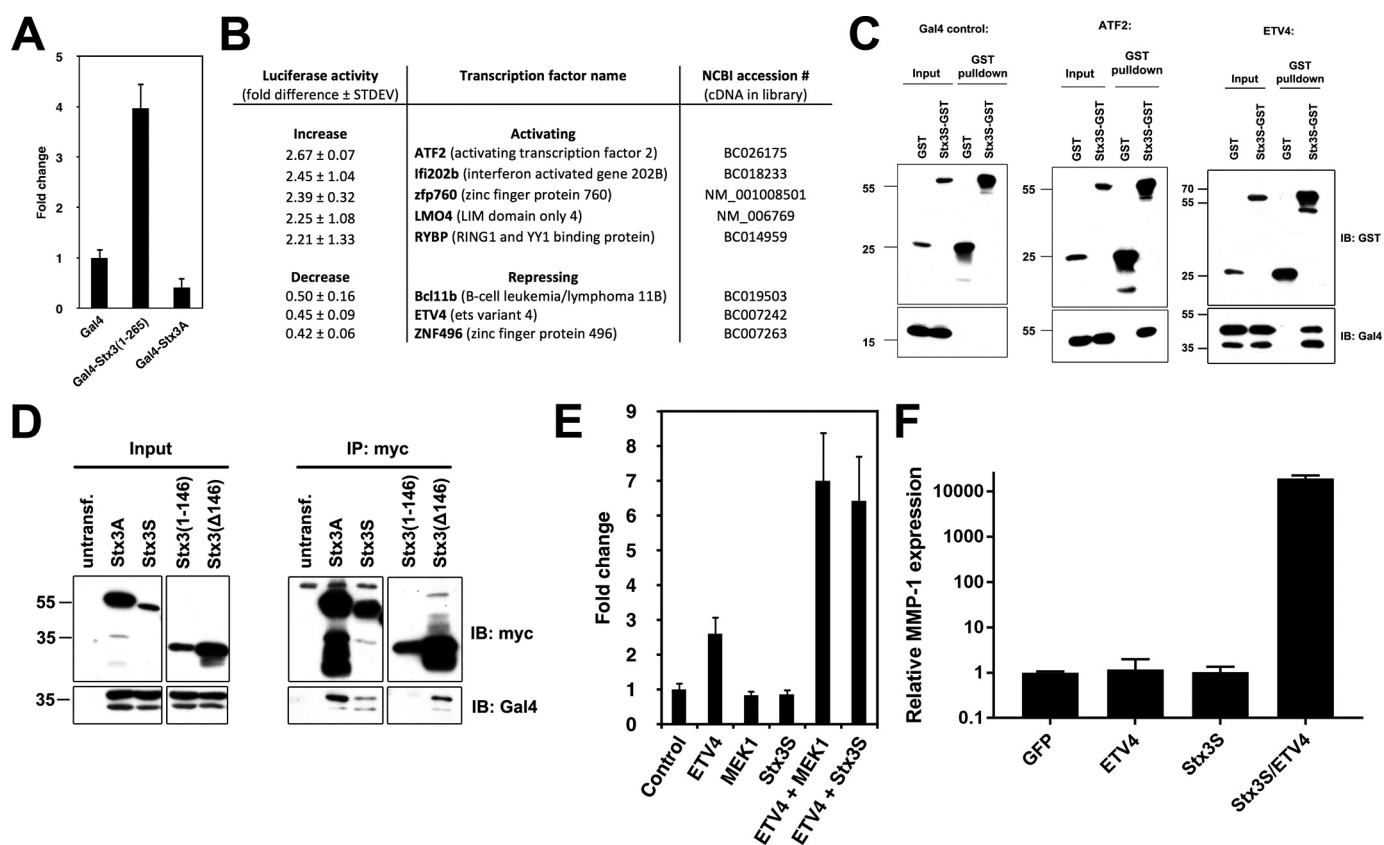


Figure 4. Stx3S acts as a transcriptional co-activator of ETV4. *A*, COS-7 cells were transiently transfected with soluble Stx3 (amino acids 1–265) or membrane-anchored Stx3A fused to the DNA-binding domain of Gal4. Transcriptional activity was measured using a luciferase reporter construct containing Gal4 binding elements ($n = 3$). *B*, table showing transcription factors whose activity was most strongly altered by Stx3S in the co-activator trap screen. *C*, co-precipitation binding assay. Stx3S-GST was transiently co-expressed in HEK293T cells with either Gal4 alone, Gal4-ATF2, or Gal4-ETV4. Stx3S-GST was precipitated from lysates using glutathione-Sepharose, and interacting proteins were probed by immunoblot with an antibody against Gal4. *D*, co-precipitation binding assay. Myc-tagged Stx3A, Stx3S, or two Stx3 deletion constructs were transiently co-expressed in HEK293T cells with Gal4-ETV4. Cell lysates (Input) were immunoprecipitated (IP) with anti-Myc and analyzed by immunoblotting (IB) with antibodies against Gal4 or Myc as indicated. *E*, ETV4 luciferase reporter assay in HeLa cells. The indicated genes were expressed by transient transfection together with an ETV4-responsive luciferase reporter plasmid. A non-responsive β -galactosidase plasmid was used as an internal control, and signals were normalized to β -galactosidase activity ($n = 3$). *F*, HEK293T cells were transiently transfected with GFP (control), ETV4, Stx3S, or Stx3S/ETV4; stimulated with PMA for 4 h; and harvested for reverse transcriptase and qPCR to quantify endogenous MMP-1 expression. MMP-1 expression was normalized to GAPDH. The bars represent the means and S.E. of triplicate samples. The data are representative of three independent experiments.

in tumor cells *in vivo* and in rapidly proliferating carcinoma cells *in vitro*.

Soluble Stx3 interacts physically and functionally with transcription factors

The discovery of a soluble, nuclear-targeted isoform of Stx3 led us to hypothesize that Stx3S may function as a signaling protein that may regulate gene expression. To test this possibility, a classic Gal4-based transcriptional transactivation assay was employed (30). Constructs encoding the Gal4 DNA-binding domain fused to membrane-anchored Stx3A or cytoplasmic Stx3(1–265), respectively, were co-expressed with a reporter plasmid encoding the luciferase gene under control of a Gal4-responsive promoter. Expression of Gal4-Stx3(1–265) resulted in 4-fold transactivation over Gal4 alone or the membrane-anchored Gal4-Stx3A construct (Fig. 4A). This finding suggests that the cytoplasmic Stx3 domain either has intrinsic transcriptional activation capability and/or interacts with other transcription factors.

To identify transcription factors that may functionally interact with Stx3S, a high-throughput, cell-based screening

assay, termed “co-activator trap” was employed (31). An arrayed library of 1465 sequenced-verified plasmids coding for mouse and human transcription-related proteins fused to the Gal4 DNA-binding domain was co-expressed with a Gal4 UAS::luciferase reporter in the presence or absence of Stx3S. Several transcription factors were identified whose activity was affected by Stx3S. The top eight that exhibited the strongest co-activation or co-repression by Stx3S were selected for validation and further analysis (Fig. 4B). To confirm binding interactions, a GST–Stx3S fusion protein was expressed together with each of these transcription factors (as fusion proteins with the Gal4 DNA binding domain). Six of these eight transcription factors (ETV4, ATF2, Ifi202b, Znf496, RybP, and LMO4) co-precipitated with GST–Stx3S, indicating that they form stable complexes (Fig. 4C and Fig. S2). ETV4 and ATF2 showed the most robust interactions.

Stx3S co-activates ETV4

ETV4 was selected for further analysis because its interaction with Stx3S was very consistent and because both ETV4 and Stx3 have been shown to play roles in renal epithelial differen-

Syntaxin 3 as transcriptional regulator

tiation. ETV4 is essential for branching morphogenesis during renal development (32, 33) and associated with several epithelial cancers (15). Stx3A is highly expressed in renal tubule epithelial cells (9) and required for the establishment of epithelial cell polarity (14). Immunoprecipitation experiments with truncated Stx3 constructs revealed that the C-terminal half of Stx3 interacts with ETV4 (Fig. 4D), suggesting that the N-terminal three-helix bundle may remain available for binding to RanBP5.

To test whether Stx3S acts on ETV4-regulated promoters, a luciferase reporter gene controlled by five ETV4-binding elements was used. Constitutively active MEK1 served as a positive control, because ETV4 activity is enhanced in response to the ERK/MAP kinase signaling pathway (34). Expression of either constitutively active MEK1 or Stx3S caused a significant increase in ETV4-dependent reporter gene activity (Fig. 4E). Next, we examined whether Stx3S can regulate the expression of a native, endogenous ETV4 target gene. ETV4 has previously been shown to increase MMP-1 expression in epithelial cancers (35, 36). Expression of Stx3S together with ETV4 in HEK293T cells leads to extremely strong endogenous MMP-1 expression compared with either Stx3S or ETV4 alone (Fig. 4F). Altogether, these results demonstrate that Stx3S physically interacts with ETV4 and acts as a co-activator of ETV4-regulated transcription.

Loss of endogenous Stx3S leads to changes in gene expression and increased cell proliferation

To demonstrate a function of endogenous Stx3S, independent of its overexpression, we specifically silenced expression of Stx3S without affecting Stx3A. To achieve this, multiple shRNA sequences flanking the unique exon 9/11 border were tested in HEK293T cells. shRNA sequence #C4 led to efficient and specific knockdown of Stx3S expression and was used for all subsequent experiments (Fig. S3, A and B). Stable Caco2 and HEK293T cell lines were generated with the Stx3S-specific shRNA or scrambled control shRNA (Fig. 5A). To identify Stx3S-regulated target genes in a non-biased fashion, the gene expression profiles between Caco2 cells with silenced Stx3S expression and control Caco2 cells were compared. Numerous genes were found to be differentially regulated in the absence of endogenous Stx3S, and those genes with the largest difference are shown in Fig. 5B. Many of these affected genes are predicted to be regulated by ATF2 (37), which we had found to physically and functionally interact with Stx3S (Fig. 4, B and C). The Stx3S-dependent regulation of three of the genes predicted to be influenced by ATF2 (FNTA, KDM2B, and SART3) were confirmed with qPCR (Fig. 5C). These results indicate that loss of endogenous Stx3S leads to distinct changes in gene expression consistent with a role as a regulator of transcription factors including ATF2.

We assessed whether loss of endogenous Stx3S expression may lead to distinct cellular phenotypes. As shown in Fig. 5D, knockdown of Stx3S expression leads to an increase in cell proliferation in Caco2 cells both in media containing serum and in serum-free conditions. Increased proliferation is validated by a 75% increase of cyclin B1 (M phase)-positive staining observed in 5-day cultures (Fig. 5, E and F). No difference in apoptosis is seen by cleaved caspase-3 staining (Fig. S4). These results,

together with the finding that Stx3S expression is down-regulated in rapidly proliferating Caco2 cells (Fig. 3, A and B) and down-regulated in breast cancer tissue (Fig. 3, C and D), suggest that Stx3S may play a role in dampening proliferation of epithelial cells and may therefore be a tumor suppressor.

Soluble splice variants of other syntaxin genes

Evidence for a handful of syntaxin variants lacking transmembrane anchors has previously been reported (24, 38–42), but their functions are unknown. To understand whether a conserved mechanism may be involved in the generation of these alternative transcripts from different syntaxin genes, we analyzed the mechanisms leading to the previously reported “soluble” variants of Stx1A, Stx1B, and Stx2. Furthermore, human EST databases were searched for possible evidence of novel soluble variants of other syntaxin genes. In addition to Stx3S reported here, we identified alternative transcripts, supported by numerous ESTs, leading to novel variants of other syntaxins lacking C-terminal transmembrane anchors, including Stx4 and Stx10 (Fig. 6A). Because the nomenclature of syntaxins is frequently inconsistent, we propose to name any syntaxin variant lacking a C-terminal transmembrane anchor by appending the letter S (soluble) to the original gene name as shown in Fig. 6A.

The alternative transcripts coding for these soluble syntaxins are generated by exon skipping (Stx3S and Stx2S-1), use of an alternative 3' acceptor site (Stx1AS), use of a cryptic exon (Stx2S-2), or intron retention (Stx1BS, Stx4S, and Stx10S), respectively (Fig. 6A). In all cases, this leads to the replacement of the transmembrane domain with short, hydrophilic sequences that exhibit no apparent sequence similarity among them.

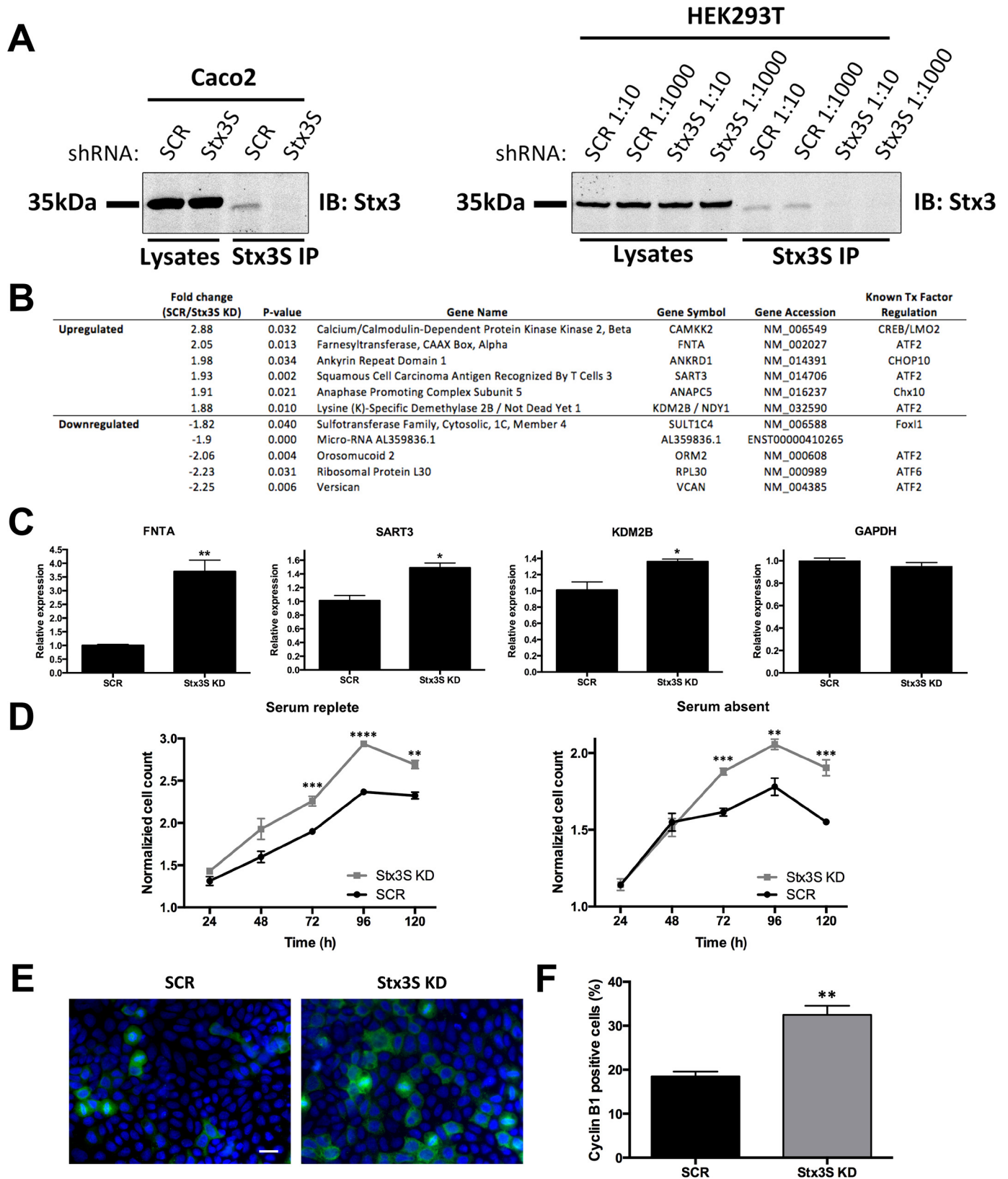
Although Stx1BS has been reported (24) to exhibit nuclear localization similar to Stx3S, no targeting information is available for the other isoforms. To investigate whether nuclear targeting may be a common feature of soluble syntaxin isoforms, Stx2S-1 and Stx2S-2 were investigated. Both isoforms target to the nucleoplasm when expressed *in vitro* (Fig. 6B). Altogether, these results suggest that mammalian syntaxin genes are commonly expressed as alternative transcripts leading to soluble isoforms that undergo nuclear targeting.

Discussion

Here we demonstrate that a novel isoform of Stx3 acts as a transcriptional regulator in the nucleus. This function requires the lack of the C-terminal transmembrane anchor because of alternative splicing to generate the soluble Stx3S. This is an unexpected, novel function for a member of the SNARE family. However, it appears likely that nuclear functions may not be unique to Stx3 but represent a characteristic that is common among many members of this SNARE family. Our finding that soluble splice variants of numerous other syntaxins exist supports this. A splice-isoform of human Stx1B (termed Stx1BS in Fig. 6A) was reported to localize to the nucleus of various tumor and non-tumor cell types (24). Stx17 has been reported to localize to the nucleus by immunohistochemistry in several cell types (43), but it is currently unknown whether this may be due to the existence of an alternatively spliced variant. A human

Stx1A splice variant (termed Stx1AS in Fig. 6A) is expressed in numerous tissues and cell types (38, 40), but its subcellular targeting has not been thoroughly investigated. We demonstrate that Stx2S-1 and Stx2S-2, two previously reported soluble vari-

ants, exhibit nuclear localization (Fig. 6B). In addition, we identified novel variants of Stx4 and Stx10 that lack transmembrane domains (Fig. 6A). Although most of the identified soluble syntaxin variants diverge from the membrane-anchored variants



Syntaxin 3 as transcriptional regulator



Figure 6. Soluble, nuclear-targeted isoforms are common among the syntaxin gene family. *A*, schematic of previously or newly identified splice variants of various syntaxin genes coding for soluble proteins lacking C-terminal transmembrane anchors. For consistency, soluble isoforms are termed here by appending the letter S. RNA splicing patterns for the canonical membrane-anchored variants are compared with splicing for the S variants. The boxes represent exons with coding regions shaded in green. C-terminal protein sequences are shown with transmembrane domains highlighted in black, and the novel sequences of S isoforms shown underlined and **bolded**. The glutamine (Q) residue that is highly conserved between all syntaxin family members is highlighted in red. Soluble isoforms human Stx1AS (originally termed Stx1C) (38), human Stx1BS (originally termed Stx1B- Δ TMD) (24), rat Stx2S-1 (originally termed Stx2C) (39), and rat Stx2S-2 (originally termed Stx2D) (39) have been described previously. The soluble isoforms human Stx3S, human Stx4S, and human Stx10S were identified in this study. *B*, immunocytochemistry of COS-7 cells transiently expressing Myc-tagged Stx2A, Stx2S-1, or Stx2S-2, respectively. The cells were stained with anti-Myc antibody (green) and DAPI (blue). The scale bars are marked in μ m.

immediately adjacent to the start of the transmembrane domain, two isoforms (Stx1AS and Stx2S-2) instead diverge immediately after a highly conserved glutamine in the middle of the SNARE motif (Fig. 6A). In the case of Stx2, both types of soluble variants exist, and both exhibit nuclear targeting (Fig. 6B). The C-terminal, hydrophilic peptide extensions of the soluble Stx splice isoforms (Fig. 6A) do not exhibit any apparent homology to each other or to other known motifs and are not required for nuclear targeting. It remains to be elucidated whether these short sequences have any function in addition to replacing the transmembrane anchors.

Stx3 has previously been found to interact with the SNARE protein SNAP-47, a member of the SNAP-25 family (44). Curiously, SNAP-47 strongly targets to the nucleoplasm when nuclear export is inhibited by leptomycin B (45). Although there is currently no known function of SNAP-47 in the nucleus, it is tempting to speculate that Stx3S and SNAP-47 may interact there physically and functionally.

We cannot formally rule out that soluble Stx3 may also have a SNARE-related function in regulating membrane fusion, *e.g.* by acting as a dominant-negative inhibitor of SNARE interactions. However, experimental experience indicates that recombinant, soluble versions of SNAREs only act as dominant-negative inhibitors at very high, artificial expression levels (46, 47). We consider it unlikely that the extremely low, endogenous expression level of Stx3S described here would affect normal SNARE function, especially given that Stx3S is targeted to the nucleus and is therefore separated from cytoplasmic SNAREs.

We found that the expression of Stx3S is up-regulated in Caco2 colon carcinoma cells as they transition from a rapidly proliferating phenotype to a fully confluent, polarized epithelial phenotype (Fig. 3, A and B). Similarly, the expression of Stx3S is higher in normal breast epithelium compared with TNBC samples (Fig. 3, C and D). TNBC, a particularly aggressive and therapy-resistant form of breast cancer, is characterized by elevated

Figure 5. Stx3S acts as a transcriptional co-activator of ATF2 and affects cell proliferation. *A*, specific knockdown of Stx3S without affecting Stx3A expression. Caco2 and HEK293T cells, respectively, were stably transduced with lentivirus delivering shRNA #C4 targeting Stx3S or scrambled control shRNA (SCR) (Fig. S3B). HEK293T cells were transduced with two different dilutions of lentivirus preparation leading to similar knockdown efficiencies. Stx3S was immunoprecipitated with a Stx3S-specific antibody. Total cell lysates and immunoprecipitates (IP) were analyzed by immunoblot with an antibody against total Stx3. *B*, effect of Stx3S knockdown on global, endogenous gene expression. Stx3S expression was knocked down in Caco2 cells using shRNA as in *A*. Gene expression was analyzed by Affymetrix microarray analysis in comparison to Caco2 cells with scrambled control shRNA. Statistically significant transcripts with the largest fold difference compared with control cells are shown in the table, including the transcription factors predicted to associate with them (last column, as projected by SABiosciences' text-mining application and the UCSC Genome Browser) (37). *C*, verification of results of select genes from microarray analysis in *B* by qPCR of the indicated genes. All genes normalized to β -actin. The bars represent the means and S.E. of triplicate samples. *, $p < 0.05$; **, $p < 0.01$ (Student's unpaired *t* test). The data are representative of three independent experiments. *D*, growth curve of Stx3S KD or shRNA scrambled control (SCR) Caco2 cells determined by CellTiter-Glo cell viability assay, normalized to 24 h reading. The growth curves were determined in the presence or absence of serum side by side. The data points represent the means and S.E. of quadruplicate samples. **, $p < 0.01$; ***, $p < 0.001$; ****, $p < 0.0001$ (Student's unpaired *t* test). *E*, representative immunocytochemistry images of 5-day cultures of SCR or Stx3S KD Caco2 cells stained for cyclin B1 (green) and DAPI (blue). Scale bar, 20 μ m. *F*, quantification of the fraction of cyclin B1-positive cells for SCR and Stx3S KD Caco2 cells. The bars represent the means and S.E. of triplicate samples. **, $p < 0.01$ (Student's unpaired *t* test).

expression of FNTA (48) and the histone demethylase KDM2B/NDY1 (49), two genes whose expression we have found to increase when Stx3S is silenced (Fig. 5, B and C). This connection is further supported with the observed increase in proliferation of Caco2 cells lacking Stx3S (Fig. 5, D–F). Altogether, these results suggest that Stx3S may regulate epithelial phenotypes important in carcinogenesis. A role in tumorigenesis has also been proposed for Stx1BS (24), which exhibits nuclear localization in human glial tumors, and its expression correlates with a worse outcome in brain tumor patients.

The low protein expression level of Stx3S observed appears to be due to proteasomal degradation (Fig. 2, H and I). Such turnover would be typical for signaling proteins and may be the reason why the nuclear localization of Stx3 and other syntaxins has previously escaped detection. Altogether, our results have uncovered a novel and unforeseen signaling pathway. Syntaxins are a conserved family of SNARE proteins involved in every intracellular membrane-trafficking step in eukaryotic cells. Signaling by soluble syntaxins may be of fundamental importance to a wide variety of cellular functions.

Experimental procedures

Cell culture and transfections

MDCK cells were cultured as described previously (50). HEK293T, HeLa, Caco2, and COS-7 cells were cultured in DMEM with 10% FBS, penicillin, and streptomycin. TurboFect (Thermo Scientific) or FuGENE 6 (Promega) were used for transient transfections according to the manufacturers' instructions. Stable MDCK cell lines were generated by transfection using calcium phosphate precipitation and selection for antibiotic resistance as previously described (14). Caco2 and HEK293T cells stably expressing shRNA against Stx3S were generated by transduction with lentiviral vectors followed by selection with puromycin.

Plasmids and mutagenesis

All Stx3 constructs are based on human Stx3 as described (14). cDNAs of full-length or truncated syntaxins were inserted into pcDNA4/TO/2× Myc/His as previously described (47). The QuikChange site-directed mutagenesis kit (Agilent Technologies) was used to generate mutations per the manufacturer's instructions.

GFP-Stx3 was constructed by insertion of the cDNA of Stx3 into pEGFP-C1 (Clontech). GST fusion proteins for mammalian expression were constructed by insertion of GST into pcDNA4/TO/Myc/His, followed by subcloning of Stx3S upstream of GST. pCMX-Gal4(DBD) encodes Gal4 DBD (amino acids 1–147) (52). pCMX-Gal4(DBD)-wtStx3 and pCMX-Gal4(DBD)-Stx3(1–265) were constructed by inserting Stx3A or Stx3(1–265) into pCMX-Gal4(DBD). Gal4(DBD) fused to various transcription factors have been described (31). Plasmids coding for mouse ETV4 pRSV-Pea3, FLAG-Pea3, and 5× Pea3-LUC were kindly provided by John Hassell (McMaster University, Hamilton, Canada). Human pFLAG-E1AF coding for ETV4 was kindly provided by Andrew Sharrocks (University of Manchester, Manchester, UK) and has been described previously (53). A plasmid encoding constitutively active MEK-1(ΔNS218E-S222D) was kindly provided by Dr. Roger

Davis (University of Massachusetts, Worcester, MA). All constructs were verified by sequencing. Plasmids encoding Stx2 splice isoforms in a pcDNA4 backbone were described previously (47).

shRNA and lentivirus

Oligonucleotides containing candidate shRNA sequences (Fig. S3A) against Stx3S were designed to have restriction sites appropriate for integration into the pGreenPuro plasmid an improved third generation of HIV-based expression lentivector (System Biosciences, CA). pGreenPuro shRNA plasmids were used with pMDG envelope and p8.91 packaging plasmids in HEK293T cells to generate lentiviral particles according to the manufacturer's instructions.

Antibodies

Hybridoma cells for the 9E10 anti-Myc epitope tag antibody were obtained from the American Type Culture Collection (Manassas, VA). Anti-β-actin (AC-15, Sigma) was used for immunoprecipitations and Western blotting; anti-Myc (4A6, Millipore) and anti-cyclin B1 (D5C10, Cell Signaling) were used for immunofluorescence. Also used were anti-GFP (JL-8, BD Bioscience), anti-GST (GE Healthcare), anti-Gal4 DBD (sc-510, Santa Cruz), anti-RanBP5 (sc-11369, Santa Cruz), and anti-Pea3 (sc-113, Santa Cruz); a mouse monoclonal antibody was developed in-house against the cytoplasmic domain of rat Stx3 (clone 1–146, licensed to EMD Millipore and available under the name MAB2258). Secondary antibodies conjugated to DyLight 488 or 594 and HRP were obtained from Thermo Scientific and Jackson ImmunoResearch Laboratories, respectively. Rabbit anti-Stx3S anti-serum was developed against a peptide specific to the C terminus of Stx3S.

Immunoprecipitation

For RanBP5 co-immunoprecipitations, MDCK cells expressing Stx3A or COS-7 cells transiently transfected with truncated Stx3 constructs were lysed in buffer containing 50 mM Hepes, pH 7.4, 150 mM potassium acetate, 0.5% Triton X-100, and a protease inhibitor mixture. Myc-tagged Stx3 was immunoprecipitated by using anti-Myc antibody 9E10 cross-linked to protein G-Sepharose using dimethyl pimelimidate. For GST-pull-downs and co-immunoprecipitations of Gal4-fusion proteins from the co-activator trap screen, HEK293T cells were transiently transfected using Turbofect and plasmids of interest. The cells were lysed in buffer containing 20 mM Tris, 1% Triton X-100, 150 mM NaCl, protease, and phosphatase inhibitors. The cells were sonicated for 15 s on ice using a probe sonicator at 20% output and 40% duty cycle. Stx3S-GST and Myc-tagged Stx3 constructs were precipitated with glutathione-conjugated Sepharose beads and anti-Myc (9E10) antibody respectively. Precipitated proteins were eluted in 2× SDS sample buffer and analyzed by SDS-PAGE and Western blotting. For endogenous Stx3S immunoprecipitations, the cells were lysed in buffer containing 25 mM Hepes, pH 7.4 (KOH-buffered), 125 mM KOAc, 2.5 mM MgOAc, 5 mM EGTA, 1 mM DTT, 0.5% Triton X-100, and protease inhibitors. Lysates were homogenized and centrifuged at 17,900 × g. Supernatants were precleared with CL2B-Sepharose (GE Healthcare) and incubated with anti-Stx3S anti-

Syntaxin 3 as transcriptional regulator

body overnight at 4 °C. Antibodies were precipitated with protein A-Sepharose, eluted in 2× SDS sample buffer and subjected to SDS-PAGE and Western blotting.

Identification of Stx3-interacting proteins by mass spectrometry

C-terminally Myc-tagged Stx3A was expressed in stably transfected, DOX-inducible MDCK cells cultured on 15-cm dishes, and uninduced cells served as a negative control. Proteins were immunoprecipitated using anti-Myc antibody (clone 9E10) covalently linked to protein G-Sepharose using dimethyl pimelimidate. Eluted proteins were analyzed by SDS-PAGE and silver staining. Identification of proteins by mass spectrometry was done as previously described (see the supporting information in Ref. 54). Briefly, excised bands were washed with 50% ethanol, 5% acetic acid containing DTT followed by alkylation with iodoacetamide. Samples were digested with trypsin and analyzed by LC-tandem mass spectrometry. Mass and CID spectra were gathered, compared with the NCBI nonredundant database, and confirmed manually.

Immunocytochemistry

MDCK or Caco2 cells were fixed in 4% paraformaldehyde for 15 min. After quenching in PBS containing 75 mM ammonium chloride and 25 mM glycine, the cells were permeabilized with PBS containing 3% BSA and 0.2% Triton X-100. The cells were incubated with primary antibodies overnight at 4 °C, followed by fluorescence-labeled (DyLight 488) secondary antibodies for 1 h at 37 °C. Images were acquired at room temperature using an Olympus IX81 microscope, a UplanSApo 60×/1.35 lens, Immersol 518 F oil (Zeiss), a Retiga EXi camera (QImaging) and IPLab software (BD Biosciences). The images were processed using Adobe Photoshop for linear histogram adjustments and to assemble composite figures. COS-7 cells were transiently transfected with pcDNA4-Stx2A-Myc, pcDNA4-Stx2S1-Myc, or pcDNA4-Stx2S2 plasmids and processed as above for immunocytochemistry.

RNA sequencing data analysis

RNA sequencing data derived from human primary breast tissue or tumor samples were downloaded from the Gene Expression Omnibus (accession no. GSE52194) and aligned to the human genome (hg19) using default settings of TopHat (v2.0.10). Because these data were generated specifically to examine differential splicing in cancer, we examined the splice pattern of Stx3 in these data ($n_{\text{NBS}} = 3$, $n_{\text{TNBC}} = 6$). Stx3 exons were counted using *htseq*, and differential exon usage was determined with the *DEXSeq* package in R. Splice reads mapping to exon 11 were filtered from TopHat's junction.bed output, merged by sample type (tumor *versus* normal), and visualized using the Integrative Genomics Viewer. Because spliced reads mapping to exon 11 align either to the junction between exons 9 and 11 or between exons 10 and 11, these junction counts represent the abundance of exon 10 exclusion and inclusion isoforms respectively.

RNA sequencing data from 95 human individuals representing 27 different tissues was obtained from the European Nucleotide Archive (study ERP003613). Tissues of interest

were imported into Illumina's BaseSpace cloud server using the SRA Import application and aligned to the human genome (hg19, RefSeq) using the TopHat Alignment application, v1.0.0. Splice junctions between exons were visualized and quantified using the Integrative Genomics Viewer Sashimi Plot, version 2.3.68. The average number of spliced reads that aligned to the junctions between exons 9 and 10 and between exons 10 and 11 represent the abundance of Stx3A. Spliced reads that aligned to the junction between exons 9 and 11 represent Stx3S.

Co-activator trap screen

This high-throughput, cell-based screening strategy to study the functional interactions of co-activators with transcription factors has been previously described in detail (31). Briefly, a sequence-verified cDNA library of ~1400 Gal4-tagged transcription factors was co-transfected with a *GAL4 UAS::luciferase* reporter and either empty vector or full-length Stx3S in HEK293T cells. The transcription factor library was purified from glycerol stocks with the NucleoSpin 96 plasmid DNA prep kit (Macherey Nagel) and spotted into 384-well plates. Library screening was done in reverse transfection format by adding serum-free DMEM containing FuGENE 6 (Promega), pG5-luc (Promega), and either pcDNA4 or Stx3S to each well. Following a 20–30-min incubation, DMEM, 20% FBS containing 10,000 HEK293T cells was added to each well. The cells were cultured for 24 h, and luciferase luminescence was measured using Britelite Plus (PerkinElmer Life Sciences) on an Analyst HT plate reader (Molecular Devices).

Luciferase assays

Gal4 transactivation assays were performed as described (30). Briefly, COS-7 cells were transiently transfected in triplicate with the different Gal4-fusion constructs, Gal4-LUC reporter, and β -galactosidase plasmid as a transfection control. The cells were lysed in luciferase lysis buffer (Promega) 48 h after transfection. Luciferase activity was measured on identical amounts of total cellular lysates using a commercial kit (Promega) and normalized to β -galactosidase activity. In addition, lysates were analyzed by Western blotting with anti-Gal4 antibodies to verify the levels of expression of the various proteins.

For ETV4 reporter assays, HEK293T or HeLa cells were plated on 96-well plates. 16 h later, the cells were transfected with the ETV4 luciferase reporter plasmid (5× Pea3 RE-LUC), and expression plasmids for ETV4, Stx3, and/or MEK1, and β -galactosidase per well. One day after transfection, the cells were lysed in passive lysis buffer (Promega), and luciferase activity was measured as described above.

RT-PCR and quantitative PCR

Total RNA was extracted from different cell types or tissue using RNAeasy Plus extraction kit (Qiagen). For RNA extraction from human kidney, the tissues were frozen in liquid nitrogen and stored at –80 °C. 30 mg of tissue was homogenized in a bullet blender (Next Advance) in buffer RLT Plus (Qiagen), and RNA was extracted as described above. For RT-PCR, 2 μ g of total RNA was reverse transcribed into cDNA using random primers and Moloney murine leukemia virus reverse transcrip-

tase (Promega) according to the manufacturer's instruction. The PCR was performed with *Pfu* Ultra for cloning or *Taq* polymerase for analytical purposes respectively. MMP-1 primers have been described (55). The following primer set was used for the identification of Stx3S, forward hStx3Sxon9_ for 5'-GGAGAAGGCACGAGATGAAA-3' and reverse hStx3Sxon11_rev 5'-GGTTGCAAGGAAACAAAGGA-3'. Stx3S was cloned from HEK293T cells using two different primer sets. Set1 was used for the initial amplification from cDNA as a template using the forward primer hStx3C_F 5'-ATGAAGGACCGTCTGGAGCAGCTG-3' and the reverse primer hStx3C_R 5'-TCATCTGAAGACAAGGGTGGCCAC-3'. The reamplification was performed with the following second set of primers hStx3C_EcoRI_for_1 5'-TTTAAA-AAGAATTCATGAAGGACCGTCTGGAGCAGCTG-3' and hStx3_NotI_rev_1 5'-TTTTTAAAGCGGCCGCTCTGAAG-ACAAGGGTGGCCACACC-3', and the PCR product was ligated into pcDNA4/TO/2×Myc/His. Stratagene Mx3000P real-time system (Agilent Technologies, Santa Clara, CA) were used for the qPCR. In addition to the aforementioned MMP-1 primer set, the following primers were used for qPCR: FNTA, forward 5'-GCAGGATCGTGGTCTTTCCA-3', reverse 5'-AACTCCTGCAGGGTCCCTTA-3'; KDM2B forward 5'-GACTTGTCGGACGTGGAGGA-3', reverse 5'-CACATGTGTCCACCCAGTC-3' (51); SART3, forward 5'-TCAATGGCAAGAAAACGGGT-3', reverse 5'-AAGCCATGGCGTACTCATCC-3'; GAPDH, forward 5'-AGCAAGAGCACAAGAGGAAGAG-3', reverse 5'-GAGCACAGGGTACTTTATTGATGG-3'; and β -actin, forward 5'-GAAGTGTGACGTTGACATCC-3', reverse 5'-ACAGACTTTCGCTCAGG-3'. Relative quantitation using the $2^{(-\Delta\Delta Ct)}$ method was used to determine gene expression.

Microarray gene expression analysis

Microarray analysis of Caco2 cells stably expressing shRNA against Stx3S was set up in triplicate. Briefly, the cells were lysed, and total RNA was isolated using the RNeasy kit from Qiagen. 5 μ g of RNA were used to produce cDNA followed by generation of biotinylated cRNA. The samples were analyzed by the University of Pennsylvania School of Medicine Microarray facility by hybridization to GeneChip Human Gene 2.0 ST arrays (Affymetrix, Santa Clara, CA). Comparisons between group means were done by a two-sided heteroscedastic Student's *t* test.

Cell viability and proliferation assays

In quadruplicate, Caco2 cells stably expressing shRNA against Stx3S were seeded in complete media. After 24 h, media were changed to serum-free or complete media. At indicated time points after changing media, wells were analyzed using the CellTiter-Glo luminescent cell viability assay (Promega, Madison, WI) per manufacturer's instructions. Statistical analysis was performed in Prism4 (GraphPad Software, La Jolla, CA).

In triplicate, Caco2 cells stably expressing shRNA against Stx3S or scrambled control were seeded in complete media. The media were changed 24 h after seeding. Five days after media change, the cells were harvested and processed as above

for immunocytochemistry using antibodies against cyclin B1 or cleaved caspase-3 and counterstained with DAPI. Positive cells were counted using FIJI software. An average of 250 cells were counted per replicate. Statistical analysis was performed in Prism4 (GraphPad Software, La Jolla, CA).

Author contributions—A. J. G., C. W., and P. B. formal analysis; A. J. G., C. W., P. B., E. R., S. H. L., J. E. B., M. X., and M. A. L. investigation; A. J. G. methodology; A. J. G., C. W., P. B., E. R., J. B. H., and T. W. writing-review and editing; J. B. H. and T. W. supervision; J. B. H. and T. W. funding acquisition; T. W. conceptualization; T. W. writing-original draft; T. W. project administration.

Acknowledgments—We thank Roger Davis (University of Massachusetts), John Hassell (McMaster University), and Andrew Sharrocks (University of Manchester) for reagents and advice.

References

- Weimbs, T., Low, S. H., Chapin, S. J., Mostov, K. E., Bucher, P., and Hofmann, K. (1997) A conserved domain is present in different families of vesicular fusion proteins: a new superfamily. *Proc. Natl. Acad. Sci. U.S.A.* **94**, 3046–3051 [CrossRef Medline](#)
- Weimbs, T., Mostov, K., Low, S. H., and Hofmann, K. (1998) A model for structural similarity between different SNARE complexes based on sequence relationships. *Trends Cell Biol.* **8**, 260–262 [CrossRef Medline](#)
- Wickner, W., and Schekman, R. (2008) Membrane fusion. *Nat. Struct. Mol. Biol.* **15**, 658–664 [CrossRef Medline](#)
- Südhof, T. C. (2014) The molecular machinery of neurotransmitter release (Nobel lecture). *Angewandte Chemie* **53**, 12696–12717 [CrossRef Medline](#)
- Rothman, J. E. (2014) The principle of membrane fusion in the cell (Nobel lecture). *Angewandte Chemie* **53**, 12676–12694 [CrossRef Medline](#)
- Hong, W. (2005) SNAREs and traffic. *Biochim. Biophys. Acta* **1744**, 120–144 [CrossRef Medline](#)
- Low, S. H., Chapin, S. J., Weimbs, T., Kömüves, L. G., Bennett, M. K., and Mostov, K. E. (1996) Differential localization of syntaxin isoforms in polarized Madin–Darby canine kidney cells. *Mol. Biol. Cell* **7**, 2007–2018 [CrossRef Medline](#)
- Delgrossi, M. H., Breuza, L., Mirre, C., Chavrier, P., and Le Bivic, A. (1997) Human syntaxin 3 is localized apically in human intestinal cells. *J. Cell Sci.* **110**, 2207–2214 [Medline](#)
- Li, X., Low, S. H., Miura, M., and Weimbs, T. (2002) SNARE expression and localization in renal epithelial cells suggest mechanism for variability of trafficking phenotypes. *Am. J. Physiol. Renal Physiol.* **283**, F1111–F1122 [CrossRef Medline](#)
- Low, S. H., Marmorstein, L. Y., Miura, M., Li, X., Kudo, N., Marmorstein, A. D., and Weimbs, T. (2002) Retinal pigment epithelial cells exhibit unique expression and localization of plasma membrane syntaxins which may contribute to their trafficking phenotype. *J. Cell Sci.* **115**, 4545–4553 [CrossRef Medline](#)
- Weimbs, T., Low, S. H., Chapin, S. J., and Mostov, K. E. (1997) Apical targeting in polarized epithelial cells: there's more afloat than rafts. *Trends Cell Biol.* **7**, 393–399 [CrossRef Medline](#)
- Low, S. H., Chapin, S. J., Wimmer, C., Whiteheart, S. W., Kömüves, L. G., Mostov, K. E., and Weimbs, T. (1998) The SNARE machinery is involved in apical plasma membrane trafficking in MDCK cells. *J. Cell Biol.* **141**, 1503–1513 [CrossRef Medline](#)
- Kreitzer, G., Schmoranzler, J., Low, S. H., Li, X., Gan, Y., Weimbs, T., Simon, S. M., and Rodriguez-Boulant, E. (2003) Three-dimensional analysis of post-Golgi carrier exocytosis in epithelial cells. *Nat. Cell Biol.* **5**, 126–136 [CrossRef Medline](#)
- Sharma, N., Low, S. H., Misra, S., Pallavi, B., and Weimbs, T. (2006) Apical targeting of syntaxin 3 is essential for epithelial cell polarity. *J. Cell Biol.* **173**, 937–948 [CrossRef Medline](#)

Syntaxin 3 as transcriptional regulator

15. de Launoit, Y., Baert, J. L., Chotteau-Lelievre, A., Monte, D., Coutte, L., Mauen, S., Firlej, V., Degerny, C., and Verreman, K. (2006) The Ets transcription factors of the PEA3 group: transcriptional regulators in metastasis. *Biochim. Biophys. Acta* **1766**, 79–87 [Medline](#)
16. Gozdecka, M., and Breitwieser, W. (2012) The roles of ATF2 (activating transcription factor 2) in tumorigenesis. *Biochem. Soc. Trans.* **40**, 230–234 [CrossRef Medline](#)
17. Deane, R., Schäfer, W., Zimmermann, H. P., Mueller, L., Görlich, D., Prehn, S., Ponstingl, H., and Bischoff, F. R. (1997) Ran-binding protein 5 (RanBP5) is related to the nuclear transport factor importin- β but interacts differently with RanBP1. *Mol. Cell. Biol.* **17**, 5087–5096 [CrossRef Medline](#)
18. Fasshauer, D., Sutton, R. B., Brunger, A. T., and Jahn, R. (1998) Conserved structural features of the synaptic fusion complex: SNARE proteins reclassified as Q- and R-SNAREs. *Proc. Natl. Acad. Sci. U.S.A.* **95**, 15781–15786 [CrossRef Medline](#)
19. Sutton, R. B., Fasshauer, D., Jahn, R., and Brunger, A. T. (1998) Crystal structure of a SNARE complex involved in synaptic exocytosis at 2.4 Å resolution. *Nature* **395**, 347–353 [CrossRef Medline](#)
20. Bock, J. B., Matern, H. T., Peden, A. A., and Scheller, R. H. (2001) A genomic perspective on membrane compartment organization. *Nature* **409**, 839–841 [CrossRef Medline](#)
21. Dulubova, I., Sugita, S., Hill, S., Hosaka, M., Fernandez, I., Südhof, T. C., and Rizo, J. (1999) A conformational switch in syntaxin during exocytosis: role of munc18. *EMBO J.* **18**, 4372–4382 [CrossRef Medline](#)
22. Ibaraki, K., Horikawa, H. P., Morita, T., Mori, H., Sakimura, K., Mishina, M., Saisu, H., and Abe, T. (1995) Identification of four different forms of syntaxin 3. *Biochem. Biophys. Res. Commun.* **211**, 997–1005 [CrossRef Medline](#)
23. Martín-Martín, B., Nabokina, S. M., Lazo, P. A., and Mollinedo, F. (1999) Co-expression of several human syntaxin genes in neutrophils and differentiating HL-60 cells: variant isoforms and detection of syntaxin 1. *J. Leukocyte Biol.* **65**, 397–406 [CrossRef Medline](#)
24. Pereira, S., Massacrier, A., Roll, P., Vérine, A., Etienne-Grimaldi, M. C., Poitelon, Y., Robaglia-Schlupp, A., Jamali, S., Roedel-Trevisiol, N., Royer, B., Pontarotti, P., Lévêque, C., Seagar, M., Lévy, N., Cau, P., et al. (2008) Nuclear localization of a novel human syntaxin 1B isoform. *Gene* **423**, 160–171 [CrossRef Medline](#)
25. Kudo, N., Matsumori, N., Taoka, H., Fujiwara, D., Schreiner, E. P., Wolff, B., Yoshida, M., and Horinouchi, S. (1999) Leptomycin B inactivates CRM1/exportin 1 by covalent modification at a cysteine residue in the central conserved region. *Proc. Natl. Acad. Sci. U.S.A.* **96**, 9112–9117 [CrossRef Medline](#)
26. Rodriguez-Boulan, E., and Nelson, W. J. (1989) Morphogenesis of the polarized epithelial cell phenotype. *Science* **245**, 718–725 [CrossRef Medline](#)
27. Peterson, M. D., and Mooseker, M. S. (1992) Characterization of the enterocyte-like brush border cytoskeleton of the C2BBE clones of the human intestinal cell line, Caco-2. *J. Cell Sci.* **102**, 581–600 [Medline](#)
28. Eswaran, J., Horvath, A., Godbole, S., Reddy, S. D., Mudvari, P., Ohshiro, K., Cyanam, D., Nair, S., Fuqua, S. A., Polyak, K., Florea, L. D., and Kumar, R. (2013) RNA sequencing of cancer reveals novel splicing alterations. *Sci. Rep.* **3**, 1689 [CrossRef Medline](#)
29. Horvath, A., Pakala, S. B., Mudvari, P., Reddy, S. D., Ohshiro, K., Casimiro, S., Pires, R., Fuqua, S. A., Toi, M., Costa, L., Nair, S. S., Sukumar, S., and Kumar, R. (2013) Novel insights into breast cancer genetic variance through RNA sequencing. *Sci. Rep.* **3**, 2256 [CrossRef Medline](#)
30. Vecchi, M., Polo, S., Poupon, V., van de Loo, J. W., Benmerah, A., and Di Fiore, P. P. (2001) Nucleocytoplasmic shuttling of endocytic proteins. *J. Cell Biol.* **153**, 1511–1517 [CrossRef Medline](#)
31. Amelio, A. L., Miraglia, L. J., Conkright, J. J., Mercer, B. A., Batalov, S., Cavett, V., Orth, A. P., Busby, J., Hogenesch, J. B., and Conkright, M. D. (2007) A coactivator trap identifies NONO (p54nrb) as a component of the cAMP-signaling pathway. *Proc. Natl. Acad. Sci. U.S.A.* **104**, 20314–20319 [CrossRef Medline](#)
32. Lu, B. C., Cebrian, C., Chi, X., Kuure, S., Kuo, R., Bates, C. M., Arber, S., Hassell, J., MacNeil, L., Hoshi, M., Jain, S., Asai, N., Takahashi, M., Schmidt-Ott, K. M., Barasch, J., et al. (2009) Etv4 and Etv5 are required downstream of GDNF and Ret for kidney branching morphogenesis. *Nat. Genet.* **41**, 1295–1302 [CrossRef Medline](#)
33. Kuure, S., Chi, X., Lu, B., and Costantini, F. (2010) The transcription factors Etv4 and Etv5 mediate formation of the ureteric bud tip domain during kidney development. *Development* **137**, 1975–1979 [CrossRef Medline](#)
34. O'Hagan, R. C., Tozer, R. G., Symons, M., McCormick, F., and Hassell, J. A. (1996) The activity of the Ets transcription factor PEA3 is regulated by two distinct MAPK cascades. *Oncogene* **13**, 1323–1333 [Medline](#)
35. Bosc, D. G., Goueli, B. S., and Janknecht, R. (2001) HER2/Neu-mediated activation of the ETS transcription factor ER81 and its target gene MMP-1. *Oncogene* **20**, 6215–6224 [CrossRef Medline](#)
36. Keld, R., Guo, B., Downey, P., Gulmann, C., Ang, Y. S., and Sharrocks, A. D. (2010) The ERK MAP kinase-PEA3/ETV4-MMP-1 axis is operative in oesophageal adenocarcinoma. *Mol. Cancer* **9**, 313–313 [CrossRef Medline](#)
37. Kent, W. J., Sugnet, C. W., Furey, T. S., Roskin, K. M., Pringle, T. H., Zahler, A. M., and Haussler, D. (2002) The human genome browser at UCSC. *Genome Res.* **12**, 996–1006 [CrossRef Medline](#)
38. Jagadish, M. N., Tellam, J. T., Macaulay, S. L., Gough, K. H., James, D. E., and Ward, C. W. (1997) Novel isoform of syntaxin 1 is expressed in mammalian cells. *Biochem. J.* **321**, 151–156 [CrossRef Medline](#)
39. Quiñones, B., Riento, K., Olkkonen, V. M., Hardy, S., and Bennett, M. K. (1999) Syntaxin 2 splice variants exhibit differential expression patterns, biochemical properties and subcellular localizations. *J. Cell Sci.* **112**, 4291–4304 [Medline](#)
40. Nakayama, T., Mikoshiba, K., Yamamori, T., and Akagawa, K. (2003) Expression of syntaxin 1C, an alternative splice variant of HPC-1/syntaxin 1A, is enhanced by phorbol-ester stimulation in astroglia: participation of the PKC signaling pathway. *FEBS Lett.* **536**, 209–214 [CrossRef Medline](#)
41. Nakayama, T., Mikoshiba, K., Yamamori, T., and Akagawa, K. (2004) Activation of syntaxin 1C, an alternative splice variant of HPC-1/syntaxin 1A, by phorbol 12-myristate 13-acetate (PMA) suppresses glucose transport into astroglia cells via the glucose transporter-1 (GLUT-1). *J. Biol. Chem.* **279**, 23728–23739 [CrossRef Medline](#)
42. Nakayama, T., Kamiguchi, H., and Akagawa, K. (2012) Syntaxin 1C, a soluble form of syntaxin, attenuates membrane recycling by destabilizing microtubules. *J. Cell Sci.* **125**, 817–830 [CrossRef Medline](#)
43. Zhang, Q., Li, J., Deavers, M., Abbruzzese, J. L., and Ho, L. (2005) The subcellular localization of syntaxin 17 varies among different cell types and is altered in some malignant cells. *J. Histochem Cytochem.* **53**, 1371–1382 [CrossRef Medline](#)
44. Jurado, S., Goswami, D., Zhang, Y., Molina, A. J., Südhof, T. C., and Malenka, R. C. (2013) LTP requires a unique postsynaptic SNARE fusion machinery. *Neuron* **77**, 542–558 [CrossRef Medline](#)
45. Kuster, A., Nola, S., Dingli, F., Vacca, B., Gauchy, C., Beaujouan, J. C., Nunez, M., Moncion, T., Loew, D., Formstecher, E., Galli, T., and Proux-Gillardeaux, V. (2015) The Q-soluble N-ethylmaleimide-sensitive factor attachment protein receptor (Q-SNARE) SNAP-47 regulates trafficking of selected vesicle-associated membrane proteins (VAMPs). *J. Biol. Chem.* **290**, 28056–28069 [CrossRef Medline](#)
46. Weimbs, T., Low, S. H., Li, X., and Kreitzer, G. (2003) SNAREs and epithelial cells. *Methods* **30**, 191–197 [CrossRef Medline](#)
47. Low, S. H., Li, X., Miura, M., Kudo, N., Quiñones, B., and Weimbs, T. (2003) Syntaxin 2 and endobrevin are required for the terminal step of cytokinesis in mammalian cells. *Dev. Cell* **4**, 753–759 [CrossRef Medline](#)
48. Singha, P. K., Pandeswara, S., Venkatachalam, M. A., and Saikumar, P. (2013) Manumycin A inhibits triple-negative breast cancer growth through LC3-mediated cytoplasmic vacuolation death. *Cell Death Dis.* **4**, e457 [CrossRef Medline](#)
49. Kottakis, F., Foltopoulou, P., Sanidas, I., Keller, P., Wronski, A., Dake, B. T., Ezell, S. A., Shen, Z., Naber, S. P., Hinds, P. W., McNiel, E., Kuperwasser, C., and Tschlis, P. N. (2014) NDY1/KDM2B functions as a master regulator of polycomb complexes and controls self-renewal of breast cancer stem cells. *Cancer Res.* **74**, 3935–3946 [CrossRef Medline](#)
50. Low, S. H., Miura, M., Roche, P. A., Valdez, A. C., Mostov, K. E., and Weimbs, T. (2000) Intracellular redirection of plasma membrane traffick-

- ing after loss of epithelial cell polarity. *Mol. Biol. Cell* **11**, 3045–3060 [CrossRef Medline](#)
51. Vlahopoulos, S. A., Logotheti, S., Mikas, D., Giarika, A., Gorgoulis, V., and Zoumpourlis, V. (2008) The role of ATF-2 in oncogenesis. *BioEssays* **30**, 314–327 [CrossRef Medline](#)
52. Perlmann, T., and Jansson, L. (1995) A novel pathway for vitamin A signaling mediated by RXR heterodimerization with NGFI-B and NURRL. *Genes Dev.* **9**, 769–782 [CrossRef Medline](#)
53. Nishida, T., Terashima, M., Fukami, K., and Yamada, Y. (2007) Repression of E1AF transcriptional activity by sumoylation and PIASy. *Biochem. Biophys. Res. Commun.* **360**, 226–232 [CrossRef Medline](#)
54. Talbot, J. J., Shillingford, J. M., Vasanth, S., Doerr, N., Mukherjee, S., Kinter, M. T., Watnick, T., and Weimbs, T. (2011) Polycystin-1 regulates STAT activity by a dual mechanism. *Proc. Natl. Acad. Sci. U.S.A.* **108**, 7985–7990 [CrossRef Medline](#)
55. Guo, B., Sallis, R. E., Greenall, A., Petit, M. M., Jansen, E., Young, L., Van de Ven, W. J., and Sharrocks, A. D. (2006) The LIM domain protein LPP is a coactivator for the ETS domain transcription factor PEA3. *Mol. Cell. Biol.* **26**, 4529–4538 [CrossRef Medline](#)

Soluble syntaxin 3 functions as a transcriptional regulator

Adrian J. Giovannone, Christine Winterstein, Pallavi Bhattaram, Elena Reales, Seng Hui Low, Julie E. Baggs, Mimi Xu, Matthew A. Lalli, John B. Hogenesch and Thomas Weimbs

J. Biol. Chem. 2018, 293:5478-5491.

doi: 10.1074/jbc.RA117.000874 originally published online February 23, 2018

Access the most updated version of this article at doi: [10.1074/jbc.RA117.000874](https://doi.org/10.1074/jbc.RA117.000874)

Alerts:

- [When this article is cited](#)
- [When a correction for this article is posted](#)

[Click here](#) to choose from all of JBC's e-mail alerts

This article cites 55 references, 28 of which can be accessed free at <http://www.jbc.org/content/293/15/5478.full.html#ref-list-1>